Ultrafast Structural Dynamics of the Fe-Pnictide Parent Compound BaFe$_2$As$_2$

L. Rettig,[1,*] S. O. Mariager,[1] A. Ferrer,[2,1] S. Grübel,[1] J. A. Johnson,[1] J. Rittmann,[3,1] T. Wolf,[4]
S. L. Johnson,[2] G. Ingold,[1,5] P. Beaud,[1,5] and U. Staub[1]

[1]*Swiss Light Source, Paul Scherrer Institut, CH-5232 Villigen PSI, Switzerland*
[2]*Institute for Quantum Electronics, Physics Department, ETH Zürich, CH-8093 Zürich, Switzerland*
[3]*Ecole Polytechnique Fédérale de Lausanne, Laboratoire de Spectroscopie Ultrarapide,*
ISIC, FSB, CH-1015 Lausanne, Switzerland
[4]*Karlsruhe Institute of Technology, Institut für Festkörperphysik, D-76021 Karlsruhe, Germany*
[5]*SwissFEL, Paul Scherrer Institut, CH-5232 Villigen PSI, Switzerland*
(Received 3 November 2014; published 13 February 2015)

Using femtosecond time-resolved x-ray diffraction we investigate the structural dynamics of the coherently excited A_{1g} phonon mode in the Fe-pnictide parent compound BaFe$_2$As$_2$. The fluence dependent intensity oscillations of two specific Bragg reflections with distinctly different sensitivity to the pnictogen height in the compound allow us to quantify the coherent modifications of the Fe-As tetrahedra, indicating a transient increase of the Fe magnetic moments. By a comparison with time-resolved photoemission data, we derive the electron-phonon deformation potential for this particular mode. The value of $\Delta\mu/\Delta z = -(1.0-1.5)$ eV/Å is comparable with theoretical predictions and demonstrates the importance of this degree of freedom for the electron-phonon coupling in the Fe pnictides.

In the Fe pnictides, the complex interplay of the electronic, spin, orbital, and lattice degrees of freedom leads to the emergence of a complex phase diagram, including structural transitions, nematic order, spin-density wave (SDW) phases, and high-temperature superconductivity. These phases emerge for electron and hole doping, but also for isovalent doping and external pressure [1,2]. The electronic structure and the magnetic properties depend very sensitively on the exact shape and size of the Fe-As tetrahedra, where an important degree of freedom is the pnictogen height h above the Fe layers, which changes the Fe-As tetrahedra angle α [see Fig. 1(a)]. A high sensitivity of the Fe magnetic moments on the pnictogen height with a rate of 6.8 μ_B/Å has been predicted [3], signifying a strong magnetostructural coupling [2,4,5]. Similarly, an increase of the electron-phonon (e-ph) coupling strength has been found in calculations including magnetic ordering [6,7]. Indeed, a universal relation between the Fe-As tetrahedra angle and the superconducting critical temperature T_c has been proposed for the Fe pnictides [2,8], underlining the importance of structural degrees of freedom in these compounds.

The role of e-ph coupling for the mechanism of superconductivity in the Fe pnictides is still controversial. The average e-ph coupling constant has been found to be relatively weak both experimentally [9–11] and theoretically [7,12] with $\lambda \lesssim 0.35$, insufficient to explain the high critical temperatures found in the pnictides in a conventional pairing scheme. However, due to the strong interplay of structural and magnetic degrees of freedom, a few phonon modes with enhanced magnetostructural coupling

could still play an important role in the superconducting pairing mechanism [5,13].

One such mode is the Raman active A_{1g} mode at the zone center corresponding to a displacement of the As ions perpendicular to the Fe layers with $\hbar\omega \approx$ 22 meV [Fig. 1(a)]. This mode directly modulates the pnictogen height h and thereby the Fe-As tetrahedra angle α. Coherent excitation of this mode has recently been observed using femtosecond (fs) time-resolved optical
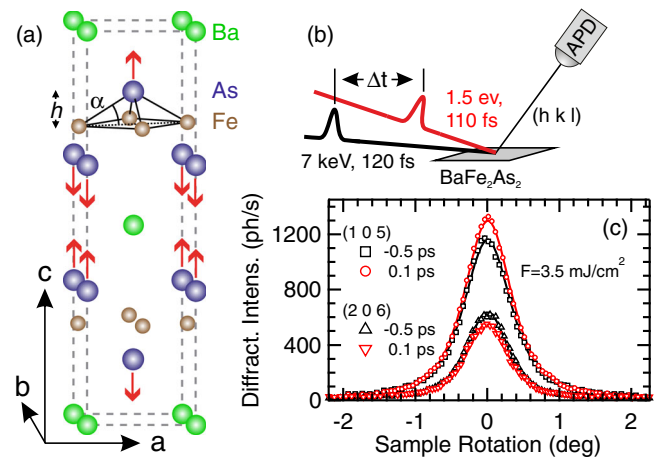

FIG. 1 (color online).   (a) Unit cell of BaFe$_2$As$_2$ with an Fe-As tetrahedron indicated. Red arrows show the atomic displacements of the A_{1g} phonon mode, which modulates the Fe-As tetrahedra angle α. (b) Sketch of the experimental geometry. (c) Time-resolved rocking curves of the (1 0 5) and (2 0 6) reflections before (black) and at 100 fs after excitation (red).

spectroscopy [14], and time-resolved THz experiments were interpreted in terms of a transient resurrection of the magnetically ordered state during the coherent oscillations [15]. In addition, using time- and angle-resolved photoemission spectroscopy, a strong modulation of the chemical potential by the coherent A_{1g} mode has been observed [16,17]. These observations demonstrate a significant coupling of the A_{1g} mode to both the electronic and the spin system, which is also the subject of recent theoretical investigations [13,18,19].

So far, no quantitative information about the ultrafast structural motions of the Fe-As lattice has been available. Structural information is crucial for determining the coupling of the various degrees of freedom to this coherent mode, and previous estimates of the structural displacement amplitudes relied solely on theoretical considerations. As such, even the direction of the displacive excitation towards smaller or larger tetrahedra angle α is controversial in the literature. Some papers argue that the excitation leads to a larger Fe-As distance and an increase of α [15,17], while a recent theoretical investigation predicts a transient resurrection of the SDW state for a decrease in α [19].

In this Letter, we investigate the structural dynamics of the coherently excited A_{1g} mode in the Fe-pnictide parent compound $BaFe_2As_2$ using fs time-resolved x-ray diffraction. We observe the fluence dependent intensity oscillations of two specific Bragg reflections with opposite sensitivity to the pnictogen height. Calculations of the structure factor allow us to quantify the coherent displacement and oscillation amplitudes, yielding a transient increase of the tetrahedra angle α as large as 0.7°, compatible with a transient increase of the Fe magnetic moment. In addition, by comparing our results to the transient chemical potential shift observed in time- and angle-resolved photoemission spectroscopy, we are able to quantify the e-ph deformation potential and determine the e-ph coupling constant $\lambda_{A_{1g}}$ for this particular mode.

High-quality single crystals of $BaFe_2As_2$ were grown by a self-flux method [20]. Time-resolved x-ray diffraction experiments were performed at the hard x-ray FEMTO slicing facility at the Swiss Light Source [21] in an asymmetric diffraction configuration [22] [Fig. 1(b)]. The (0 0 1) surface of the cleaved $BaFe_2As_2$ single crystal was kept at $T = 140$ K during the measurements using a cryogenic nitrogen blower. This is above the Néel temperature $T_N \approx 134$ K and avoids a splitting of the Bragg peaks due to the orthorhombic distortion below T_N. The sample was excited at a 1 kHz repetition rate by 1.55 eV laser pulses with a duration of ~110 fs full-width at half maximum (FWHM). The sliced x-ray pulses (~120 fs FWHM) were incident on the sample at a grazing angle of $\alpha_i = 0.43°$, matching the x-ray penetration depth to the optical penetration depth of ~25 nm at the x-ray energy of 7 keV (260 photons/pulse at 2 kHz). The x-ray beam was focused to 10 μm vertically and 300 μm

horizontally to ensure a homogenous excitation of the probed volume. The overall time resolution was ~160 fs. The diffracted x-ray photons were detected by a fast avalanche photodiode (APD).

Time-resolved rocking curves for a rotation about the sample surface normal for the (1 0 5) and (2 0 6) lattice reflections are shown in Fig. 1(c) before (black) and at $t = 0.1$ ps after excitation (red). The rocking curves are well described by a squared Lorentzian function (lines), which demonstrates the homogeneity and high crystal quality of the sample. The two reflections show a distinctly different response to the pump pulse: Whereas the (1 0 5) reflection shows a significant increase after excitation, the (2 0 6) reflection is decreased by the pump pulse. This indicates an ultrafast increase of the Fe-As tetrahedra angle α due to the displacive excitation of the coherent A_{1g} mode (see below). Both peak position and width remain constant for both peaks for up to ~1 ps, indicating little influence of strain for these early times [23].

The normalized pump-induced intensity change $\Delta I/I$ of the (1 0 5) reflection is shown in Fig. 2(a) as a function of pump-probe delay. After the ultrafast increase of the diffraction signal by ~5% at t_0 within the experimental time resolution [24], the signal shows an exponential decay with a sub-ps timescale, superimposed by an oscillatory component. Such a behavior is typical for the displacive excitation of a coherent phonon. An abrupt change of the atomic potential landscape induced by the pump laser results in a new position of the potential minimum and leads to coherent oscillations around this new minimum [27]. The exponential decay of the intensity change reflects the relaxation of the excited energy potential surface, as well as the influence of lattice heating, which influences the x-ray signal via the Debye-Waller effect.
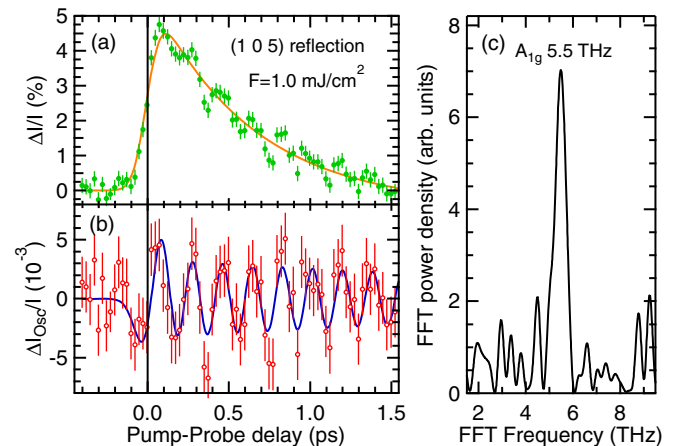

FIG. 2 (color online). (a) Pump-induced change of the peak intensity of the (1 0 5) reflection as a function of pump-probe delay for an absorbed fluence of $F = 1.0$ mJ/cm². (b) Oscillatory component after subtracting an exponential fit to the data [orange line in (a)]. The blue line is a fit of a damped oscillator. (c) FFT spectrum of the data in (b), showing a clear peak at 5.5 THz.

The oscillatory component is extracted from the data by subtracting an exponential step function (orange line), and is shown in Fig. 2(b). A fit of a damped cosine function to the data yields a frequency of $f = 5.46(9)$ THz, which is corroborated by the clear peak in the fast Fourier transformation (FFT) of the data shown in Fig. 2(c), centered at 5.5 THz. This value is in very good agreement with the frequency of the coherent A_{1g} mode observed by time-resolved optical [14], THz [15], and photoemission [16,17,28] experiments. In addition, the phase $\Phi = -1.1(2)\pi$ of the oscillation, which is very close to a pure cosinelike excitation, is consistent with models for the displacive excitation of coherent phonons (DECP) [27].

For a more quantitative analysis of the coherent phonon oscillations, the pump-induced intensity change is shown for various fluences as a function of pump-probe delay for the (1 0 5) and (2 0 6) reflections in Figs. 3(a) and 3(b), respectively. In agreement with our observation in Fig. 1(c), the two reflections show an opposite behavior after excitation, with a displacive increase in intensity for (1 0 5) and a decrease for (2 0 6), superimposed by the coherent oscillations of the A_{1g} mode.

In order to determine the amplitudes of displacement and oscillations, we model the transient change in the

diffraction signal for $t > 0$ by the following expression for a displacively excited mode, consisting of a displacive and an oscillatory component:

$$\Delta I/I_0(t) = A_{\text{disp}}e^{(-t/\tau_{\text{disp}})} + A_{\text{osc}}\cos(\omega t + \Phi)e^{(-t/\tau_{\text{osc}})}. \quad (1)$$

Here, A_{disp} and A_{osc} are the amplitudes of displacive and oscillatory components, τ_{disp} and τ_{osc} the relaxation time-scales of the displacive and oscillatory part, and ω and Φ the frequency and phase of the oscillation, respectively. In order to take the finite temporal resolution of the experiment into account, Eq. (1) is convolved by a Gaussian profile with 160 fs FWHM. Because of the limited time window of the data in Fig. 3, the frequency and phase of the oscillations have been fixed at the values determined from Fig. 2.

Fits of the data to Eq. (1) are shown in Fig. 3 as lines and reproduce the data very nicely. Figure 4 summarizes the amplitudes for the displacive and oscillatory components A_{disp} and A_{osc} as solid and open symbols, and for the (1 0 5) (red) and (2 0 6) (black) reflection, respectively. Both components show a linear behavior for low fluences ($F < 2$ mJ/cm^2), and saturate for the largest fluences. Remarkably, the amplitudes of the oscillatory and displacive components agree very well within the accuracy of the experiment, as expected from the DECP model of coherent phonon excitation [27,29]. The larger error bars for A_{osc} are due to the deconvolution with the limited time resolution, which suppresses the experimentally observed oscillation amplitudes [24]. The saturation behavior observed for the highest pump fluences indicates a nonlinear response of the excited atomic potential to the electronic excitation level or anharmonicities in the atomic potential [30,31].
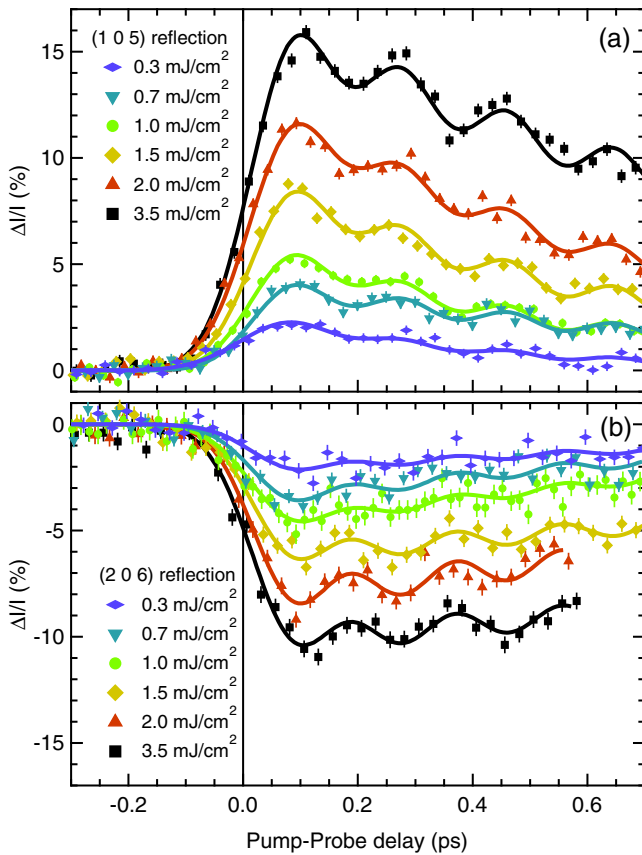

FIG. 3 (color online). Pump-induced change of the peak intensity for (a) the (1 0 5) reflection and (b) the (2 0 6) reflection for various absorbed pump fluences. Lines are fits to equation (1).
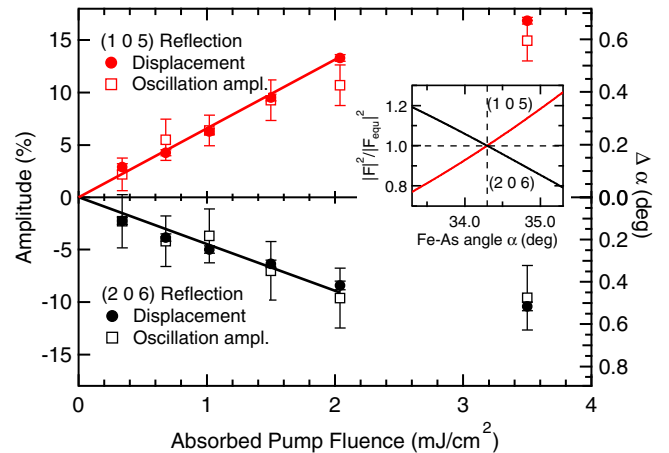

FIG. 4 (color online). Displacement amplitudes A_{disp} (circles) and oscillation amplitudes A_{osc} (squares) for the (1 0 5) (red) and (2 0 6) (black) reflections, derived from the fits in Fig. 3. Error bars are 95% confidence intervals, and lines are linear fits. Inset: Calculated normalized diffraction intensity of the (1 0 5) (red) and (2 0 6) (black) reflections as a function of Fe-As tetrahedra angle α. The vertical line marks the equilibrium position.

In order to relate the amplitudes to the microscopic atomic displacements and the modification of the Fe-As tetrahedra, we calculate the diffraction intensities of the (1 0 5) and (2 0 6) reflections as a function of the Fe-As tetrahedra angle α in the kinematic approximation [24]. The calculated normalized intensities are shown in the inset of Fig. 4 and nicely reproduce the opposite slope of the two reflections with respect to α. We find a relative intensity change of $+24.8\%$/deg for the (1 0 5) reflection, and -20.2%/deg for the (2 0 6) reflection. Comparison with the experimental amplitudes allows us to quantitatively determine the average atomic displacement induced by the coherent A_{1g} mode (right axis of Fig. 4). For the highest fluence of $F = 3.5$ mJ/cm^2, we find displacement and oscillation amplitudes as large as $\Delta\alpha = 0.68°$, corresponding to a maximal displacement $(A_{\mathrm{disp}} + A_{\mathrm{osc}})$ of the As atoms by $\Delta h = 7$ pm, more than 5% of the equilibrium pnictogen height. A linear fit at low fluences yields an amplitude of 0.26(1) deg/mJcm^{-2} [1.32(6) pm/mJcm^{-2}] for the (1 0 5) reflection, and 0.22(2) deg/mJcm^{-2} [1.12(11) pm/mJcm^{-2}] for the (2 0 6) reflection. The slight difference of the values found for the two reflections could be due to the limits of the kinematic approximation, or could indicate further structural components in the coherent oscillations beyond the vertical motion of the As coordinate [16].

The quantification of the absolute oscillation amplitude of the coherent A_{1g} mode offers important insight into the interplay of structural and electronic degrees of freedom, by comparison to the imprint of the same coherent phonon oscillation on the electronic structure observed by time-resolved photoemission spectroscopy. Yang *et al.* [17] report a coherent modulation of the chemical potential of ~ 40–50 meV/mJcm^{-2}. Comparing this with the structural information obtained here, and taking the different probe depth of the x-rays and the photoemission process into account [24], we estimate a deformation potential of the As A_{1g} mode of $\Delta\mu/\Delta\alpha = -(0.05$–0.08$)$ eV/deg or $\Delta\mu/\Delta z = -(1.0$–1.5$)$ eV/Å. This value is in reasonable agreement with the deformation potentials predicted by density functional theory for variation of the As height in various FeAs compounds [6,13,19,32,33], which are on the order of $dE/dz \sim 1.5$–2 eV/Å. The deformation potential is also comparable to the deformation potential of the coherent A_{1g} mode in Bismuth [34].

The e-ph deformation potential allows us to determine the e-ph coupling constant for the A_{1g} mode, which is related to the electronic deformation potential as [13]

$$\lambda_{A_{1g}} = \frac{1}{4 M_{\mathrm{As}} \omega_{A_{1g}}^2} N(E_F) \left(\frac{dE}{dz}\right)^2, \qquad (2)$$

where M_{As} is the As atomic mass, $\omega_{A_{1g}}$ the A_{1g} phonon frequency, and $N(E_F)$ the electronic density of states at the Fermi level. Using $N(E_F) \sim 2$–5 states/(eV formula unit)

from density functional theory [32], we obtain $\lambda_{A_{1g}} = 0.05$–0.30. This value for λ is in the same range as the total e-ph coupling constant λ_{tot} in BaFe$_2$As$_2$, as predicted theoretically [7], and measured by time-resolved optics and photoemission [10,11]. The total e-ph coupling is the sum of the coupling to all modes in the system. Thus, our finding of $\lambda_{A_{1g}} \sim \lambda_{\mathrm{tot}}$ indicates that the A_{1g} mode plays a major role for the e-ph coupling in BaFe$_2$As$_2$.

Finally, the observation of a displacive excitation towards larger pnictogen height and larger tetrahedra angles α implies an ultrafast increase of the Fe magnetic moments [2–5]. These enhanced magnetic moments could, in principle, be responsible for an ultrafast resurrection of the SDW order [15]. However, the atomic displacement at the fluence of $F \approx 0.5$ mJ/cm^2 based on band structure calculations [3] yields a maximal increase of the magnetic moment of $0.08\mu_B$, which corresponds to a relative change of $\sim 11\%$ [35]. This leads to an increase of T$_N$ by ~ 20 K, if we consider the ratio of the SDW transition temperature and the Fe magnetic moments of 200–250 K/μ_B observed in Ba$_{1-x}$K$_x$Fe$_2$As$_2$ [35] and BaFe$_2$(As$_{1-x}$P$_x$)$_2$ [36]. Given the fact that indication of a transient magnetic ordering has also been observed > 100 K above T_N [15], the increased magnetic moments cannot be solely responsible for a resurrection of SDW order, but the transiently modified nesting properties of the band structure also need to be considered [15].

In conclusion, using time-resolved x-ray diffraction, we investigated the coherent structural dynamics of the displacively excited A_{1g} phonon mode oscillations in BaFe$_2$As$_2$. Based on structure factor calculations, we determine the absolute oscillation and displacement amplitudes, and the direction of the modulation. Comparison of the absolute oscillation amplitude of the As coordinate to time-resolved photoemission experiments allows us to determine the A_{1g} deformation potential $\Delta\mu/\Delta z = -(1.0$–1.5$)$ eV/Å. An estimate of the e-ph coupling constant underlines the importance of this structural degree of freedom in the Fe pnictides. Our findings are consistent with a transient increase of the Fe magnetic moment, which, however, is predicted to be too small to explain a transient resurrection of the SDW phase in BaFe$_2$As$_2$.

Note added.—Recently, we became aware of a related study by S. Gerber et al. on arXiv.org (arXiv:1412.6842), which presents data in agreement with our observations.

———————————

*Corresponding author.
laurenz.rettig@psi.ch

[1] I. I. Mazin, Nature (London) **464**, 183 (2010).
[2] D. C. Johnston, Adv. Phys. **59**, 803 (2010).
[3] Z. P. Yin, S. Lebègue, M. J. Han, B. P. Neal, S. Y. Savrasov, and W. E. Pickett, Phys. Rev. Lett. **101**, 047001 (2008).
[4] T. Yildirim, Physica (Amsterdam) **469C**, 425 (2009).
[5] T. Egami, B. V. Fine, D. Parshall, A. Subedi, and D. J. Singh, Adv. Condens. Matter Phys. **2010**, 164916 (2010).
[6] F. Yndurain and J. M. Soler, Phys. Rev. B **79**, 134506 (2009).
[7] L. Boeri, M. Calandra, I. I. Mazin, O. V. Dolgov, and F. Mauri, Phys. Rev. B **82**, 020506 (2010).
[8] C.-H. Lee, A. Iyo, H. Eisaki, H. Kito, M. T. Fernandez-Diaz, T. Ito, K. Kihou, H. Matsuhata, M. Braden, and K. Yamada, J. Phys. Soc. Jpn. **77**, 083704 (2008).
[9] L. Stojchevska, P. Kusar, T. Mertelj, V. V. Kabanov, X. Lin, G. H. Cao, Z. A. Xu, and D. Mihailovic, Phys. Rev. B **82**, 012505 (2010).
[10] B. Mansart, D. Boschetto, A. Savoia, F. Rullier-Albenque, F. Bouquet, E. Papalazarou, A. Forget, D. Colson, A. Rousse, and M. Marsi, Phys. Rev. B **82**, 024513 (2010).
[11] L. Rettig, R. Cortés, H. S. Jeevan, P. Gegenwart, T. Wolf, J. Fink, and U. Bovensiepen, New J. Phys. **15**, 083023 (2013).
[12] L. Boeri, O. V. Dolgov, and A. A. Golubov, Phys. Rev. Lett. **101**, 026403 (2008).
[13] F. Yndurain, Europhys. Lett. **94**, 37001 (2011).
[14] B. Mansart, D. Boschetto, A. Savoia, F. Rullier-Albenque, A. Forget, D. Colson, A. Rousse, and M. Marsi, Phys. Rev. B **80**, 172504 (2009).
[15] K. W. Kim, A. Pashkin, H. Schäfer, M. Beyer, M. Porer, T. Wolf, C. Bernhard, J. Demsar, R. Huber, and A. Leitenstorfer, Nat. Mater. **11**, 497 (2012).
[16] I. Avigo, R. Cortés, L. Rettig, S. Thirupathaiah, H. S. Jeevan, P. Gegenwart, T. Wolf, M. Ligges, M. Wolf, J. Fink, and U. Bovensiepen, J. Phys. Condens. Matter **25**, 094003 (2013).
[17] L. X. Yang et al., Phys. Rev. Lett. **112**, 207001 (2014).
[18] N. A. García-Martínez, B. Valenzuela, S. Ciuchi, E. Cappelluti, M. J. Calderón, and E. Bascones, Phys. Rev. B **88**, 165106 (2013).
[19] J. D. Lee, W. S. Yun, and S. C. Hong, New J. Phys. **16**, 043010 (2014).
[20] F. Hardy, T. Wolf, R. A. Fisher, R. Eder, P. Schweiss, P. Adelmann, H. v. Löhneysen, and C. Meingast, Phys. Rev. B **81**, 060501 (2010).
[21] P. Beaud, S. L. Johnson, A. Streun, R. Abela, D. Abramsohn, D. Grolimund, F. Krasniqi, T. Schmidt, V. Schlott, and G. Ingold, Phys. Rev. Lett. **99**, 174801 (2007).
[22] S. L. Johnson, P. Beaud, E. Vorobeva, C. J. Milne, É. D. Murray, S. Fahy, and G. Ingold, Acta Crystallogr. Sect. A **66**, 157 (2010).
[23] For $t > 2$ ps, a strain wave is observed, which shifts the peak position and width. Therefore, we limit the analysis to early times.
[24] See Supplemental Material at http://link.aps.org/supplemental/10.1103/PhysRevLett.114.067402, which includes Refs. [25,26], for details on the effect of the time resolution, the structure factor calculations and the correction for the probe penetration depth.
[25] M. Rotter, M. Tegel, and D. Johrendt, Phys. Rev. Lett. **101**, 107006 (2008).
[26] P. Beaud et al., Nat. Mater. **13**, 923 (2014).
[27] H. J. Zeiger, J. Vidal, T. K. Cheng, E. P. Ippen, G. Dresselhaus, and M. S. Dresselhaus, Phys. Rev. B **45**, 768 (1992).
[28] L. Rettig, R. Cortés, S. Thirupathaiah, P. Gegenwart, H. S. Jeevan, M. Wolf, J. Fink, and U. Bovensiepen, Phys. Rev. Lett. **108**, 097002 (2012).
[29] T. Huber, S. O. Mariager, A. Ferrer, H. Schäfer, J. A. Johnson, S. Grübel, A. Lübcke, L. Huber, T. Kubacka, C. Dornes, C. Laulhe, S. Ravy, G. Ingold, P. Beaud, J. Demsar, and S. L. Johnson, Phys. Rev. Lett. **113**, 026401 (2014).
[30] M. F. DeCamp, D. A. Reis, P. H. Bucksbaum, and R. Merlin, Phys. Rev. B **64**, 092301 (2001).
[31] D. M. Fritz et al., Science **315**, 633 (2007).
[32] D. J. Singh, Phys. Rev. B **78**, 094511 (2008).
[33] R. S. Dhaka, S. E. Hahn, E. Razzoli, R. Jiang, M. Shi, B. N. Harmon, A. Thaler, S. L. Bud'ko, P. C. Canfield, and A. Kaminski, Phys. Rev. Lett. **110**, 067002 (2013).
[34] E. Papalazarou, J. Faure, J. Mauchain, M. Marsi, A. Taleb-Ibrahimi, I. Reshetnyak, A. van Roekeghem, I. Timrov, N. Vast, B. Arnaud, and L. Perfetti, Phys. Rev. Lett. **108**, 256808 (2012).
[35] S. Avci, O. Chmaissem, D. Y. Chung, S. Rosenkranz, E. A. Goremychkin, J. P. Castellan, I. S. Todorov, J. A. Schlueter, H. Claus, A. Daoud-Aladine, D. D. Khalyavin, M. G. Kanatzidis, and R. Osborn, Phys. Rev. B **85**, 184507 (2012).
[36] J. M. Allred, K. M. Taddei, D. E. Bugaris, S. Avci, D. Y. Chung, H. Claus, C. dela Cruz, M. G. Kanatzidis, S. Rosenkranz, R. Osborn, and O. Chmaissem, Phys. Rev. B **90**, 104513 (2014).